

## Some Recent Developments in Atomic Lifetime Determinations\*

P. Hannaford and R. M. Lowe

Division of Chemical Physics, CSIRO,  
P.O. Box 160, Clayton, Vic. 3168.

### Abstract

A lifetimes technique that is readily applicable to neutral and singly ionised atoms of a wide range of elements, including the highly refractory elements, is reviewed. With this technique an atomic vapour of the element under study is generated by cathodic sputtering in a low pressure rare-gas discharge and fluorescence decay signals emitted by the vapour following pulsed laser excitation are recorded directly in a fast transient digitiser. Theoretical expressions are presented for the form of the time-resolved fluorescence signal appropriate to the collisional environment of a rare-gas sputtering discharge. A summary is given of the atomic systems studied to date using this technique, and some new results for Sm and Ba are compared with recently reported results for these elements.

### 1. Introduction

Measurements of the radiative lifetimes of atomic levels, when combined with accurate branching ratio data, provide the most reliable means of determining *absolute* atomic transition probabilities, and consequently are of prime importance in many fields such as atomic physics, plasma physics, astrophysics and spectrochemical analysis. Until recently, however, little reliable lifetime data have been available for many of the elements, particularly the highly refractory elements in the second and third transition series (see e.g. Fuhr *et al.* 1978, 1980). The major problem with determining lifetimes for these elements is the difficulty in obtaining an atomic vapour or atomic beam, as temperatures in excess of 2000 K, or even 3000 K in certain cases, are required to produce a vapour pressure of around  $10^{-5}$  Torr ( $\sim 10^{11}$  atoms  $\text{cm}^{-3}$ ; 1 Torr = 133 Pa) by conventional thermal means. Similarly, few lifetime data have been available for singly ionised atoms, which are of special interest to astrophysicists since these ions are often the dominant species in the solar photosphere and other stellar atmospheres.

During the past seven years we have developed a rapid and direct lifetimes method (Hannaford and Lowe 1981, 1983a) that is readily applicable to neutral and singly ionised atoms of almost any solid element in the periodic table, including the highly refractory elements. The method makes use of cathodic sputtering in a low pressure rare-gas discharge to generate an atomic vapour of the element under study, a pulsed

\* Paper presented at the Specialist Workshop on Excited and Ionised States of Atoms and Molecules, Strathgordon, Tasmania, 3-7 February 1986.

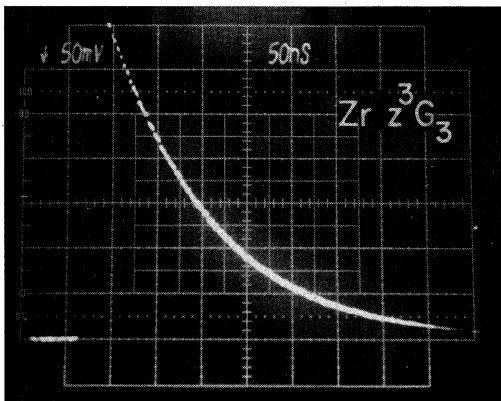


Fig. 1. Single-shot oscilloscope trace of a laser-induced fluorescence decay signal recorded for the  $z^3G_3$  level of Zr I in a sputtering discharge at 0.4 Torr Ne. The horizontal time scale is 50 ns per large division.

tunable dye laser to excite the sputtered atoms selectively to the required energy level, and a fast photomultiplier coupled to a transient digitiser (or oscilloscope) to capture the fluorescence decay signals emitted by the excited atoms. In this way it is possible to observe the fluorescence decay signals from a single laser shot directly on an oscilloscope (Fig. 1). The total time taken to accumulate a fluorescence decay curve and analyse the data in a microcomputer is less than one minute.

With the sputtering method of vaporisation the element under study is made the cathode of a low pressure rare-gas discharge and subjected to bombardment by energetic rare-gas ions formed in the cathode fall region of the discharge. Atoms of the cathode material are consequently ejected from the cathode surface with high kinetic energy and then rapidly thermalised by elastic collisions in the rare gas. As the sputtered atoms move away from the cathode, they may become excited or ionised in the discharge. Cathodic sputtering thus provides a simple and convenient means of producing relatively high steady-state number densities ( $\sim 10^{11} \text{ cm}^{-3}$  or greater) of neutral metal atoms, singly ionised atoms, and metastable atoms or ions, and the combination of this technique with pulsed laser excitation allows relatively easy access to a wide range of energy levels for almost any solid element. Although simple routine checks are required for possible effects of collisional depopulation by the rare gas and radiation trapping, such effects are rarely important for the usual operating conditions of the discharge. The method is applicable to level lifetimes in the range 3 ns to a few microseconds and the accuracy is typically 2–5%. To date, lifetime determinations have been completed for over 350 levels in elements ranging from the refractory metals V, Y, Zr, Nb, Mo, Ir, Pt and U to the more volatile elements Na, Al, Ca, Cr, Fe, Cu, Ag, Au, Ba and Sm.

A similar lifetimes method has been developed by Lawler and coworkers at the University of Wisconsin (Duquette *et al.* 1981). A feature of their method is that the sputtered vapour is allowed to expand through a small nozzle into an evacuated scattering chamber to form an effusive atomic beam. This allows measurements to be made in an essentially collision-free environment, though the number density of metal atoms in the scattering chamber and hence the signal-to-noise is reduced. A number of other lifetime measurements on refractory elements, based on laser-induced fluorescence, have also been reported in recent years. Groups at Berlin (Kwiatkowski *et al.* 1981) and Kiel (Rudolph and Helbig 1982*a*) have used electron bombardment or high temperature filaments to thermally produce an atomic beam of the element of interest, and Poulsen *et al.* (1981) at Aarhus have used charge exchange of fast ion

beams to generate a beam of neutral refractory metal atoms. These various methods have increased greatly the range of atomic systems in which lifetime measurements have been made in recent years.

In Section 2 we present a theoretical treatment of the form of the time-resolved fluorescence signal appropriate to the collisional environment of a rare-gas discharge. Section 3 briefly describes the experimental details of our lifetimes method. In Section 4 we summarise the systems studied to date and finally in Section 5 we discuss areas for future study.

## 2. Time-resolved Fluorescence in a Collision Environment

In the following treatment we apply the theory of the Hanle effect, as developed by Carrington and Corney (1971), to the case of time-resolved atomic fluorescence. The expression for the time-dependent intensity of fluorescent light emitted by an ensemble of atoms following excitation by a short pulse of light may be written as the trace of the product of two operators

$$I(t) = \text{Tr}\{\rho_e(t)M\}, \quad (1)$$

where  $\rho_e(t)$ , the excited state density matrix, describes the time evolution of the ensemble of excited state atoms and  $M$  is a monitoring operator. It is convenient to expand  $\rho_e(t)$  and  $M$  in terms of irreducible spherical tensor operators  $T_q^k$ :

$$\rho_e(t) = \sum_{k,q} \rho_q^k(t) T_q^{k\dagger}, \quad M = \sum_{k,q} M_q^k T_q^{k\dagger}, \quad (2a, b)$$

where  $k$  is a quantum number that takes the values 0, 1 and 2, and  $q$  is a projection quantum number that runs from  $k$  to  $-k$ . For the simplifying case of (i) very short excitation pulses (at time  $t = 0$ ), (ii) broad line and weak pumping excitation conditions, (iii) atoms having zero nuclear spin (no hyperfine structure), and (iv) an optically thin atomic vapour,  $\rho_q^k(t)$  takes the form

$$\rho_q^k(t) = \rho_q^k(0) \exp\{-(\Gamma^k + i\omega)t\}, \quad (3)$$

where  $\Gamma^k = \tau^{-1} + N\bar{v}\sigma_{\text{coll}}^k$  is the relaxation rate of the  $2^k$  multipole moment,  $\tau$  is the mean radiative lifetime of the excited state,  $N$  is the number density of the collision partner (rare-gas atoms),  $\bar{v}$  is the mean relative velocity of the colliding species, and  $\sigma_{\text{coll}}^k$  is the (velocity-averaged) cross section for collisional relaxation in the excited state. Here also  $\omega = g_J \mu_B B/\hbar$  is the Larmor precessional frequency in some external magnetic field  $B$ , where  $g_J$  is the Landé splitting factor of the excited state and  $\mu_B$  is the Bohr magneton. The multipole components of the initial density matrix and the monitoring operator are given by

$$\rho_q^k(0) = (-1)^{J_i+J_f+1} 3 E_q^k \begin{Bmatrix} k & 1 & 1 \\ J_i & J_e & J_e \end{Bmatrix}, \quad (4a)$$

$$M_q^k \propto (-1)^{J_i+J_f+1} 3 U_q^k \begin{Bmatrix} k & 1 & 1 \\ J_f & J_e & J_e \end{Bmatrix}, \quad (4b)$$

where  $J_i$ ,  $J_e$  and  $J_f$  are the angular momenta of the initial, excited and final states

of the atom in the excitation-fluorescence sequence  $J_i \rightarrow J_e \rightarrow J_f$ , while  $E_q^k$  and  $U_q^k$  are tensors that specify the polarisations of the exciting light  $e$  and the detected fluorescent light  $u$  respectively:

$$E_q^k = \sum_{\mu=-1}^1 e_\mu (e_{\mu-q})^* (-1)^{1+\mu} (2k+1)^{\frac{1}{2}} \begin{pmatrix} 1 & 1 & k \\ \mu & q-\mu & -q \end{pmatrix}, \quad (5a)$$

$$U_q^k = \sum_{\mu=-1}^1 u_\mu (u_{\mu-q})^* (-1)^{1+\mu} (2k+1)^{\frac{1}{2}} \begin{pmatrix} 1 & 1 & k \\ \mu & q-\mu & -q \end{pmatrix}. \quad (5b)$$

The  $e_\mu$  (and  $u_\mu$ ) are components of the unit vectors  $e$  (and  $u$ ) in the spherical basis defined by

$$e_{\pm 1} = \mp (e_x \pm i e_y) / 2^{\frac{1}{2}}, \quad e_0 = e_z. \quad (6a, b)$$

Combining equations (1)–(4) we obtain the following expression for the multipole expansion of the fluorescence intensity:

$$I(t) \propto \sum_{k,q} (-1)^q E_q^k U_{-q}^k W^k \exp\{-(\Gamma^k + i q\omega)t\}, \quad (7)$$

where the anisotropy factors  $W^k$  are given by

$$W^k = (-1)^{2J_e + J_i + J_f} (2J_e + 1)^2 \begin{Bmatrix} k & 1 & 1 \\ J_i & J_e & J_e \end{Bmatrix} \begin{Bmatrix} k & 1 & 1 \\ J_f & J_e & J_e \end{Bmatrix}. \quad (8)$$

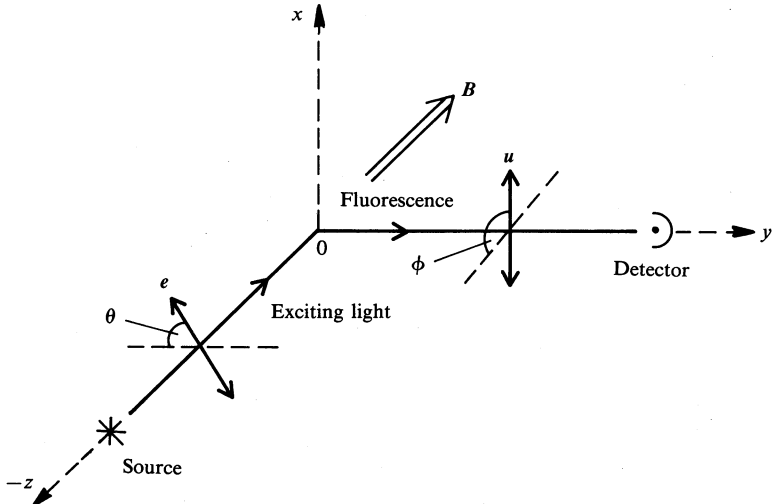


Fig. 2. Excitation-detection geometry using linear polarisers. Here  $B$  is an external magnetic field assumed to be in the (axial)  $z$  direction.

For the geometry in Fig. 2 (linear polarisations and axial magnetic field), the only non-vanishing multipole components are  $k = 0$  and  $2$ , and equation (7) reduces to

$$I(t) \propto \frac{1}{3} W^{(0)} e^{-\Gamma^{(0)} t} - \frac{1}{6} W^{(2)} [(3 \cos^2 \phi - 1) + 3 \sin^2 \phi \cos\{2(\omega t + \theta)\}] e^{-\Gamma^{(2)} t}. \quad (9)$$

The first ( $k = 0$ ) term represents the *population* of the excited state, and the second ( $k = 2$ ) term, which is angular dependent and contains a time-oscillatory component, represents the *alignment*.

When there is no polariser in the fluorescence detection channel (as is the case in most lifetime experiments), an integration is taken over the angle  $\phi$ , and equation (9) becomes

$$I(t) \propto \frac{1}{3} W^{(0)} e^{-\Gamma^{(0)} t} - \frac{1}{12} W^{(2)} [1 + 3 \cos\{2(\omega t + \theta)\}] e^{-\Gamma^{(2)} t}. \quad (10)$$

Fig. 3 shows theoretical time-resolved fluorescence curves computed from equation (10) for  $J_i = 3 \rightarrow J_e = 4 \rightarrow J_f = 3$  transitions and (axial) magnetic fields of 0, 0.5 and 5 G (1 G  $\equiv 10^{-4}$  T) (and other parameters as given in the caption). It can be seen that for the chosen conditions Zeeman beats arising from fields of the order of the Earth's field are sufficient to noticeably affect the shape of the decay signal and thus influence the measured lifetime. Hence it is important to eliminate stray fields, especially when the beat period is around an order of magnitude longer than the lifetime. In the absence of magnetic fields ( $\omega = 0$ ), equation (10) reduces to

$$I(t) \propto \frac{1}{3} W^{(0)} e^{-\Gamma^{(0)} t} - \frac{1}{6} W^{(2)} (3 \cos^2 \theta - 1) e^{-\Gamma^{(2)} t}. \quad (11)$$

For sputtering fluorescence cells of the type used in this work, the radiating atoms are in the environment of a rare gas (usually neon) at pressures of the order of 0.1–1 Torr, where the collision frequency ( $\sim 10^6$ – $10^7$  s $^{-1}$ ) may be comparable with the radiative decay rate of the excited state. The cross sections for depopulation of an excited state by collisions with rare-gas atoms  $\sigma_{\text{coll}}^{(0)}$  are usually very much smaller than the 'hard-sphere' cross sections, whereas the cross sections for destruction of the alignment by collisions  $\sigma_{\text{coll}}^{(2)}$  are usually comparable with or larger than the hard-sphere values. It is clear from equation (11) that the effect of disalignment collisions can be eliminated by setting the angle of polarisation of the exciting light  $\theta$  to the magic angle  $\arccos(\sqrt{\frac{1}{3}}) = 54.7^\circ$ . The fluorescence decay curve is then characterised by a single decay constant  $\Gamma^{(0)}$ , corresponding to the decay of the population only. This is illustrated in Fig. 4, which shows theoretical fluorescence decay curves computed from equation (11) for  $J_i = 0 \rightarrow J_e = 1 \rightarrow J_f = 0$  transitions and  $\theta$  values of 0°, 30°, 54.7° and 90° (and other parameters as given in the caption). Any shortening of the lifetime due to depopulation collisions can be easily eliminated by determining  $\Gamma^{(0)}$  at a number of rare-gas pressures and extrapolating to zero pressure.

If the excited level has hyperfine structure and the splittings  $\omega_{F_e, F'_e}$  are sufficiently small that they are spanned by the Fourier spread in frequencies associated with the duration of the excitation pulse, pairs of nondegenerate sublevels belonging to different hyperfine levels  $F_e, F'_e$  may be excited coherently and the fluorescence decay signals may exhibit beats, even in the absence of a magnetic field. The zero-field time-resolved fluorescence signal is then given by an expression of the form (see e.g. Luyperf and Van Craen 1977)

$$I(t) \propto (-1)^{J_i - J_f} \sum_{k, q, F_e, F'_e} (-1)^q E_q^k U_{-q}^k V^k \exp\{-(\Gamma^k + i\omega_{F_e, F'_e})t\}, \quad (12)$$

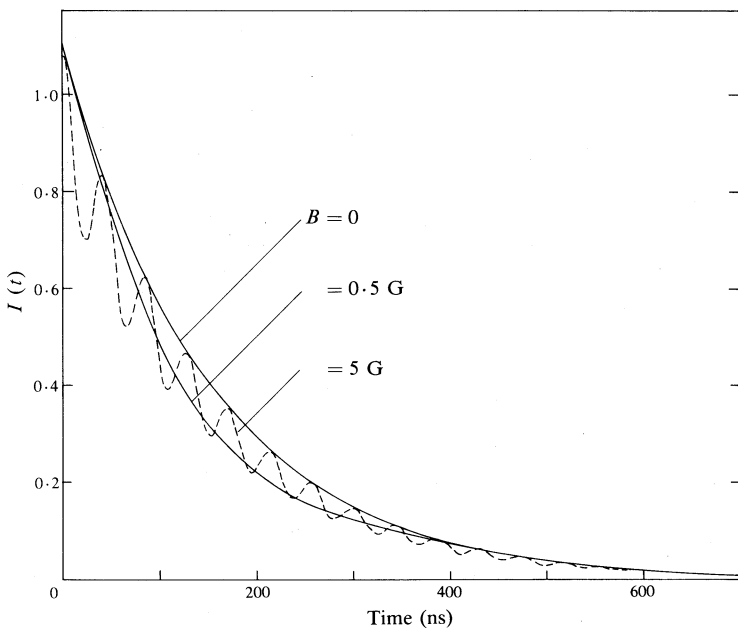


**Fig. 3.** Effect of Zeeman beats on calculated fluorescence decay curves for various values of the magnetic field  $B$  and the following conditions:  $J_i = 3 \rightarrow J_e = 4 \rightarrow J_f = 3$ , the geometry in Fig. 2, an axial magnetic field (along  $0z$ ), no polariser in the detection channel,  $\tau = 150 \text{ ns}$ ,  $g_J = 1.66$ , and no collisions.

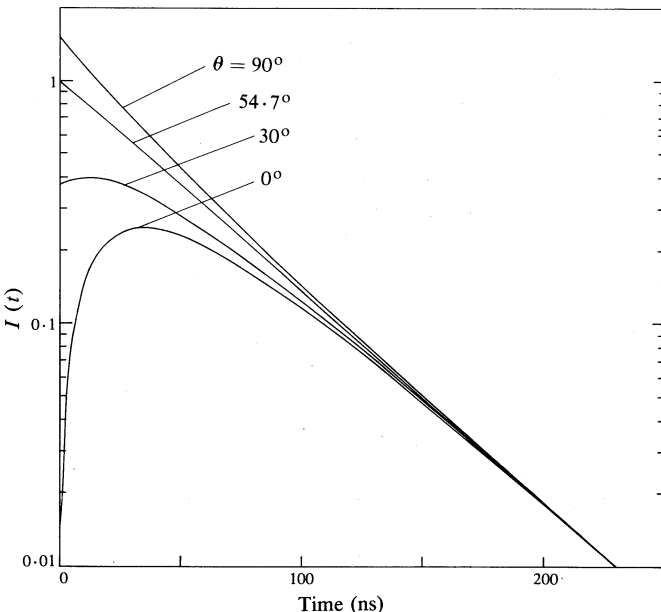


**Fig. 4.** Effect of collisional depolarisation on calculated fluorescence decay curves for different values of the polarisation angle  $\theta$  and the following conditions:  $J_i = 0 \rightarrow J_e = 1 \rightarrow J_f = 0$ , the geometry in Fig. 2, no polariser in the detection channel, neon gas at 1 Torr and 300 K,  $\tau = 50 \text{ ns}$ ,  $\sigma_{\text{coll}}^{(2)} = 100 \text{ \AA}^2$  and  $\sigma_{\text{coll}}^{(0)} = 0$ .

where the anisotropy factor  $V^k$  is now

$$V^k = (2F_e + 1)(2F'_e + 1) \begin{Bmatrix} k & F_e & F'_e \\ I & J_e & J'_e \end{Bmatrix}^2 \begin{Bmatrix} k & 1 & 1 \\ J_i & J_e & J'_e \end{Bmatrix} \begin{Bmatrix} k & 1 & 1 \\ J_f & J_e & J'_e \end{Bmatrix}, \quad (13)$$

and  $I$  is the nuclear spin. For the geometry in Fig. 2, and when there is no polariser in the fluorescence detection channel, equation (12) reduces to

$$I(t) \propto (-1)^{J_i - J_f} \sum_{F_e, F'_e} \left\{ \frac{1}{3} V^{(0)} e^{-I^{(0)} t} - \frac{1}{6} V^{(2)} (3 \cos^2 \theta - 1) \exp(-i \omega_{F_e, F'_e} t) e^{-I^{(2)} t} \right\}. \quad (14)$$

Thus setting  $\theta$  to the magic angle  $54.7^\circ$  also eliminates any hyperfine (or fine) structure beats, as well as effects of disalignment collisions.

### 3. Experimental

A schematic diagram of our experimental arrangement for determining atomic lifetimes is shown in Fig. 5. A detailed description of the various components has been reported elsewhere (Hannaford and Lowe 1983a), and only a brief account, including some recent modifications, is presented here.

The sputtering fluorescence cell consists of a Pyrex housing with side-arms, containing silica windows for transmission of the exciting and fluorescent radiation, and a demountable Pyrex base with tungsten pins which are connected to the anode and cathode. The cathode, which contains the element to be sputtered, is usually in the form of a thin wire of about 1 mm diameter. The sputtering discharge is operated in a pulsed mode (typically 10 Hz repetition rate and 3 ms pulse width) at pressures between 0.1 and 1 Torr of neon or argon. Neon is normally preferred since any collisional depopulation effects are usually smallest for this gas (see Fig. 6). The laser pulse is fired a few ms after each discharge pulse, in order to allow the fluorescence signals to be detected at a time after discharge species and emission from the discharge have decayed away, but before all of the sputtered metal atoms have diffused out of the observation region. A synchronised mechanical chopper protects the photomultiplier from intense emission which may occur during the discharge pulse.

The pulsed dye laser (Molelectron DL 200/300 pumped by a 400 kW nitrogen laser) produces pulses of 2–4 ns duration and about 10 GHz bandwidth (1 GHz with an intracavity etalon), spanning a wavelength range (including frequency doubling with KDP crystals) of 258–860 nm. The photomultiplier in the fluorescence detection channel is an RCA 1P28A/V1 with a base designed to provide high linearity at peak anode currents up to 10 mA. The photomultiplier is coupled to a 1 GHz transient digitiser (Tektronix 7912 AD, with 7A29 vertical amplifier and 7B10 time base), which records and integrates successive fluorescence decay signals under the control of a microcomputer. The time response of the total detection system, as measured by the response to single-photon pulses, is less than 2 ns (FWHM) with a fall time (90–10%) of about 3 ns. The decay region of the integrated fluorescence signal is computer-fitted to a single exponential by a weighted least-squares analysis to yield the required lifetime.

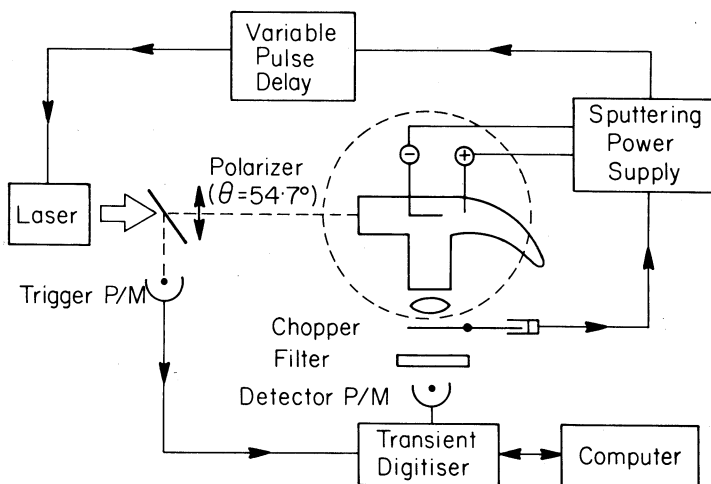


Fig. 5. Schematic diagram of the experimental arrangement for time-resolved fluorescence measurements of atomic lifetimes.

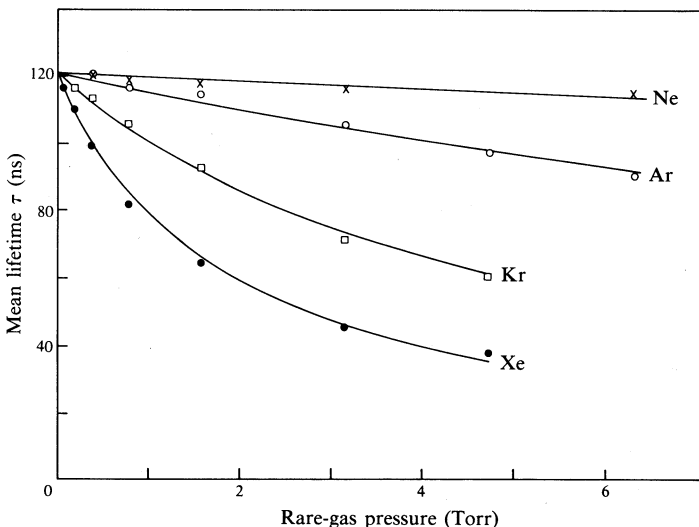


Fig. 6. Dependence of the measured lifetime of the  $z^3G_3$  level of ZrI on pressure for various rare gases.

The exciting laser light is polarised at the magic angle  $\theta = 54.7^\circ$  to eliminate effects due to collisional disalignment and hyperfine (or fine) structure quantum beats (see Section 2). Stray magnetic fields are cancelled to less than 5 mG by three pairs of Helmholtz coils in order to eliminate Zeeman beats. All measurements are made over a range of pressures of rare gas to check for collisional depopulation (see e.g. Fig. 6) and over a range of atom densities (discharge currents) to check for radiation trapping. Determinations have now been completed for over 350 levels in 18 elements and the results show that collisional depopulation is insignificant in about 90% of the cases studied; in the remaining 10% of cases the effects could be simply corrected by extrapolating the measured decay constant to zero rare-gas pressure.

When determining very short lifetimes ( $< 5$  ns) it is necessary to make allowance for the duration of the exciting laser pulse. This may be accomplished by recording separately the excitation pulse shape and numerically convoluting this recorded pulse with exponentials of varying decay constant to arrive at the best fit to the experimental data. An example of this convolution procedure is shown in Fig. 7. In practice, however, our recorded fluorescence decay curves generally have very high signal-to-noise, and it is usually sufficient to apply the usual least-squares analysis to the purely exponential region in the lower part of the decay curves (below the arrow in Fig. 7).

For levels with lifetimes longer than about 15 ns the uncertainties in the measured lifetimes are typically  $\pm 2\%$ , provided no correction is required for collisional depopulation. These uncertainties originate predominantly from nonlinearities in the photomultiplier plus transient digitiser detection system. For levels with lifetimes shorter than about 15 ns, additional uncertainties can arise from the effects of residual ringing in the photomultiplier assembly and the finite fall time of the exciting laser pulse. The actual uncertainty for these levels depends on the lifetime and increases to about  $\pm 10\%$  for lifetimes around 3 ns.

#### 4. Lifetime Results

The initial system selected for detailed lifetime measurements was atomic zirconium. This is a typical example of a highly refractory element, requiring temperatures in excess of 2000 K to vapourise by thermal methods. A semi-log plot of a fluorescence decay curve for one of the Zr levels is shown in Fig. 8.

Our 1981 lifetime results for Zr (Table 1, column 4) were found to be shorter, by factors of three to four, than the only other direct lifetime values reported at that time (beam sputtering results, column 3) and also shorter, by similar factors, than values deduced from the approximate arc-emission transition probabilities of Corliss and Bozman (1962). Many of these lifetimes have now been checked by other groups (columns 5, 6 and 7), also using laser-induced fluorescence methods, and their results are generally in good agreement with ours. Similar discrepancies have since been found in the beam sputtering results for Y, Pt and Ir (see e.g. Hannaford and Lowe 1983a). These discrepancies apparently originate from the non-selective nature of the beam-sputtering excitation process (i.e. the excitation that occurs during ejection of atoms from a target subjected to pulsed ion bombardment), and the effect of cascading and spectral impurity processes that can result.

The systems for which detailed lifetime measurements have been completed to date are summarised in Table 2. Measurements have also been made on a limited number of levels in Na, Al, Ca, Cr, Fe, Cu, Ag, Au, Ba and U (see Hannaford and Lowe 1983a and Tables 3 and 5 of this paper for details). Table 2 also gives the systems for which transition probabilities (or oscillator strengths) have been determined from the measured lifetimes, using measured branching ratios, and systems in which these transition probabilities have been applied in order to make precision determinations of solar abundances. The branching ratios in most cases were determined by W. Whaling (California Institute of Technology) using the 1 m Fourier Transform spectrometer at Kitt Peak (Brault 1976), and the solar abundances by N. Grevesse and E. Biémont (Institut d'Astrophysique, University of Liège) using solar data taken from the Jungfraujoch Solar Atlas (Delbouille *et al.* 1973).

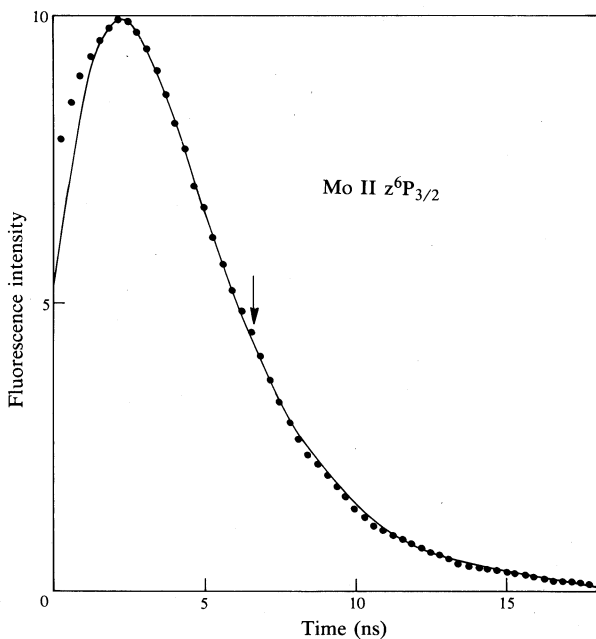


**Fig. 7.** Fluorescence decay curve recorded for the Mo II  $z^6P_{3/2}$  level in a sputtering discharge at 0.3 Torr Ne. The solid curve represents a convolution of the recorded laser excitation pulse with an exponential of decay constant  $(3.00 \text{ ns})^{-1}$ . A least-squares analysis of the region below the arrow yields  $\tau = 3.1 \text{ ns}$ .

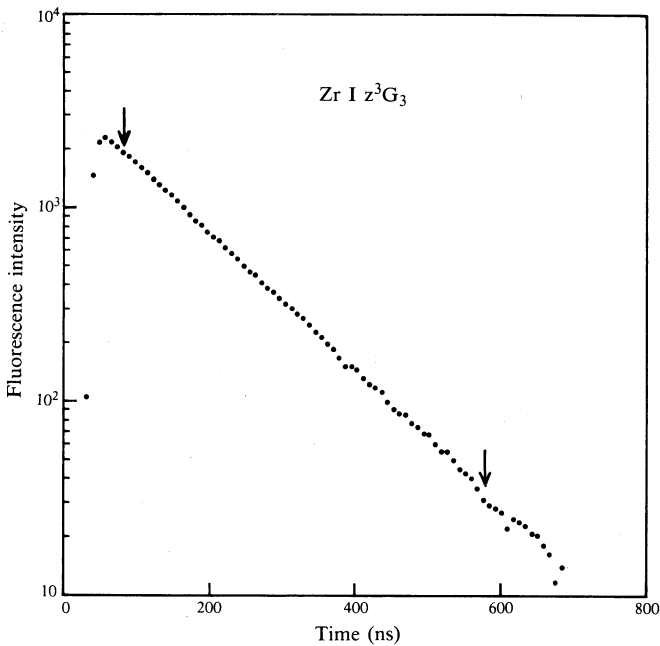


**Fig. 8.** Semi-log plot of the fluorescence decay signal for the  $z^3G_3$  level of Zr I. The sputtering discharge was operated at 0.4 Torr Ne, and the signal was accumulated over 64 laser shots. The slope of the region between the arrows yields  $\tau = 123 \text{ ns}$ .

Table 1. Comparison of lifetime results for Zr I (in ns)

Level	Energy (cm <sup>-1</sup> )	Beam sputtering	CSIRO <sup>C</sup>	Aarhus <sup>D</sup>	Laser-induced fluorescence Wisconsin <sup>E</sup>	Kiel <sup>F</sup>	CSIRO <sup>G</sup>
$z^3G_3$	21849	440(25) <sup>A</sup>	123(2)		124(6)		
$z^3G_4$	22144	380(15) <sup>A</sup>	111(2)		118(9)		
$z^3G_5$	22564	450(25) <sup>A</sup>	107(2)	118(5)	112(6)		
$y^5G_2$	25630		12.3(3)		12.0(6)	12.3(9)	
$y^5G_3$	25972		13.3(3)		13.7(7)	13.0(9)	
$y^5G_4$	26343	41(2) <sup>B</sup>	13.1(3)		13.6(7)	13.8(1.0)	
$y^5G_5$	26766	40(2) <sup>B</sup>	13.3(3)		12.8(7)	12.6(9)	12.9(2)
$y^5G_6$	27215		12.0(5)		11.1(6)		11.3(3)
$y^3G_3$	25730		16.2(3)		16.3(8)	16.0(1.1)	
$y^3G_4$	26012		21.5(4)		21.5(1.1)	17.1(1.2)	21.5(4)
$y^3G_5$	26434		27.6(6)		28.8(1.4)		

<sup>A</sup> Ramanujam (1977).<sup>B</sup> Andersen *et al.* (1978).<sup>C</sup> Hannaford and Lowe (1981).<sup>D</sup> Poulsen *et al.* (1981).<sup>E</sup> Duquette *et al.* (1982).<sup>F</sup> Rudolph and Helbig (1982 *b*).<sup>G</sup> Hannaford and Lowe (1983 *a*).

Table 2. Summary of systems studied in detail in this program

Transition probabilities  $A$  are determined from lifetimes  $\tau$  and branching ratios  $R$  using the relationship  $A = R/\tau$

System	Atomic lifetimes: number of levels studied	Transition probabilities: no. of transitions	Solar abundance
Zr I	59 <sup>A, B, C</sup>	38 <sup>B</sup>	Ref. <sup>B</sup>
Zr II	25 <sup>A, B, C</sup>	31 <sup>B</sup>	Ref. <sup>B</sup>
Y I	34 <sup>D, E</sup>	154 <sup>E</sup>	Ref. <sup>E</sup>
Y II	14 <sup>E</sup>	66 <sup>E</sup>	Ref. <sup>E</sup>
Pt I	15 <sup>F</sup>		
Ir I	25 <sup>G</sup>	27 <sup>G</sup>	
Mo I	56 <sup>H</sup>	570 <sup>H</sup>	Ref. <sup>I</sup>
Mo II	15 <sup>J</sup>		
Fe II	13 <sup>K</sup>		
VI	39 <sup>L</sup>	208 <sup>L</sup>	Ref. <sup>L</sup>
Nb II	20 <sup>M</sup>		Ref. <sup>M</sup>
Sm I	28 <sup>N</sup>		

<sup>A</sup> Hannaford and Lowe (1981).<sup>B</sup> Biémont *et al.* (1981).<sup>C</sup> Hannaford and Lowe (1983 *a*).<sup>D</sup> Hannaford and Lowe (1982).<sup>E</sup> Hannaford *et al.* (1982).<sup>F</sup> Gough *et al.* (1982).<sup>G</sup> Gough *et al.* (1983).<sup>H</sup> Whaling *et al.* (1984).<sup>I</sup> Biémont *et al.* (1983).<sup>J</sup> Hannaford and Lowe (1983 *b*).<sup>K</sup> Hannaford and Lowe (1983 *c*).<sup>L</sup> Whaling *et al.* (1985).<sup>M</sup> Hannaford *et al.* (1985).<sup>N</sup> Hannaford and Lowe (1985).

**Table 3.** Radiative lifetimes and oscillator strengths for first  $^2P$  levels of Cu, Ag and Au

Excited level	Energy ( $\text{cm}^{-1}$ )	Lifetime (ns)	Resonance line $\lambda$ (nm)	Branching ratio	Oscillator strength Exp. <sup>D</sup>	Theory <sup>E</sup>
Cu I						
$4^2\text{P}_{1/2}$	30535	7.4(2) <sup>A</sup>	327.4	0.988 <sup>C</sup>	0.215(6)	0.214
$4^2\text{P}_{3/2}$	30784	7.1(2) <sup>A</sup>	324.7	0.984 <sup>C</sup>	0.439(12)	0.432
Ag I						
$5^2\text{P}_{1/2}$	29552	6.8(3) <sup>A</sup>	338.3	1.0	0.253(11)	0.214
$5^2\text{P}_{3/2}$	30473	6.3(2) <sup>A</sup>	328.1	1.0	0.513(16)	0.445
Au I						
$6^2\text{P}_{1/2}$	37359	6.0(1) <sup>B</sup>	267.6	0.98(1) <sup>B</sup>	0.176(3)	0.158
$6^2\text{P}_{3/2}$	41174	4.6(2) <sup>B</sup>	242.8	0.911(4) <sup>B</sup>	0.351(15)	0.360

<sup>A</sup> Hannaford and Lowe (1983a).<sup>B</sup> Hannaford *et al.* (1981).<sup>C</sup> Kock and Richter (1968).<sup>D</sup> Using lifetimes of column 3 with branching ratios of column 5.<sup>E</sup> Relativistic Hartree-Fock calculations (Migdalek and Bayliss 1978, 1979).**Table 4.** Comparison of lifetime results for some low-lying levels in Sm I

Energy ( $\text{cm}^{-1}$ )	Level <sup>A</sup>	Lifetime (ns)				Hook <sup>H</sup>
		Hanle effect	Delayed coinc. <sup>D</sup>	CSIRO <sup>E</sup>	Hannover <sup>F</sup>	
$4f^66s6p$						
16691	$7D_1$			1710(100)	1450(200)	
17462	$5G_2$				122(9)	~1800
17811	$7F_0$			342(10)		
17770	$7F_1$	38(4) <sup>B</sup>		157(5)	165(10)	260
17190	$7F_2$			1020(100)	1200(130)	1100(100)
18986	$5F_1$			308(15)	41.6(2.5)	330(20)
$4f^55d6s^2$						
18076	$7H_2$			450(50)	158(5)	480(20)
18949	$7H_3$			308(10)	345(22)	
18475	$7F_1$	69(4)		71(2)	61(5)	78
18788	$7F_2$			128(5)	127(8)	
19777	$7G_3$		41(2)	40(2)		40
20713	$7G_4$	34(3) <sup>C</sup>	36(2)	33(1)		
20091	$5F_1$	44(4) <sup>C</sup>	49(3)	47(2)		
23244	$7G_1$				59.2(3.0)	~270
						450

<sup>A</sup> Designation according to Blaise *et al.* (1969).<sup>B</sup> Laser level-crossing forward scattering and laser Hanle effect (Brand *et al.* 1980).<sup>C</sup> Handrich *et al.* (1969).<sup>D</sup> Blagoev *et al.* (1977).<sup>E</sup> Hannaford and Lowe (1985).<sup>F</sup> Kulina and Rinkleff (1985).<sup>G</sup> Present work.<sup>H</sup> Deduced from relative oscillator strength hook data of Penkin and Komarovskii (1976), using the normalising factor  $18 \times 10^{-5}$  determined by Blagoev *et al.* (1977).

The lifetimes and oscillator strengths for the first  $^2P$  levels of copper, silver and gold are of particular interest since these afford a test of reported relativistic Hartree-Fock calculations (Table 3). The experimental lifetimes show the expected increasing difference between the  $^2P_{1/2}$  and  $^2P_{3/2}$  levels as the fine-structure splitting increases with atomic weight. The theoretical oscillator strengths are in excellent agreement with the experimental values for Cu and for the  $6^2S_{1/2}-6^2P_{3/2}$  transition of Au, but there are differences of 10–15% for the two Ag transitions and for the Au  $6^2S_{1/2}-6^2P_{1/2}$  transition. It would be of interest to see if better agreement can be obtained using relativistic Dirac-Fock calculations of the type described by Grant (1986, present issue p. 649) and Dyall (1986, p. 667).

In Table 4 we compare some recent lifetime results for low-lying levels in Sm I (Hannaford and Lowe 1985) with earlier results and also with the more recent laser-induced fluorescence results of Kulina and Rinkleff (1985). The lifetimes of many of the low-lying levels in Sm I are of interest in laser spectroscopy since these levels can be excited from the ground term ( $4f^66s^2\ ^7F$ ) by transitions within the tuning range of the rhodamine dyes. In particular, the 570.7 nm ( $^7F_1-^7F_0$ ) transition has recently been used in a number of fundamental laser spectroscopic experiments, including ground state quantum beat studies (Mlynek and Lange 1979), resonance Raman enhancement experiments (Raj *et al.* 1983), heterodyne detection of radiofrequency resonances (Mlynek *et al.* 1984), polarisation switching in an optical cavity (Parigger *et al.* 1985), and nonlinear Hanle effect experiments (McLean *et al.* 1985). The only previous estimate of the lifetime of the upper level ( $^7F_0$ ,  $17811\text{ cm}^{-1}$ ) of this transition was 7 ns, which was deduced from the linewidth of laser atomic beam data [Mlynek and Lange (1979) using data of Brand (1978)]. Our measured value is 342 ns. Our results are in satisfactory agreement with those of Kulina and Rinkleff for most levels; however, there are serious discrepancies for the  $18076\text{ cm}^{-1}$  ( $^7H_2$ ) and  $18986\text{ cm}^{-1}$  ( $^5F_1$ ) levels. Our most recent measurements (Table 4, column 7) reveal further discrepancies, in the  $17462\text{ cm}^{-1}$  ( $^5G_2$ ) and  $23244\text{ cm}^{-1}$  ( $^7G_1$ ) levels. Approximate lifetime values deduced from the normalised hook data of Penkin and Komarovskii (1976) (final column) support the present results; however, it would be desirable to have an additional independent set of direct lifetime measurements for these levels in Sm I.

## 5. Future Directions

Our lifetime measurements to date have been confined almost entirely to levels that can be excited by a single transition, either from the ground state or from metastable states populated in the sputtering discharge. There is currently much interest in highly excited atomic states, and in particular in series of Rydberg states close to the ionisation potential. Very little information is available about such states in complex atoms, and it remains to be seen how closely to the ionisation potential one will be able to probe, for example, using stepwise excitation with two pulsed dye lasers or two-photon excitation with a single laser, before the effects of collisions in the rare gas or residual discharge effects become excessive.

A few preliminary measurements, using stepwise and two-photon excitation, have recently been carried out in atomic barium (Table 5, columns 5 and 6). The highest state we have studied to date is the  $6s10d\ ^1D_2$  ( $39998\text{ cm}^{-1}$ ), which is about 95% of the way to the ionisation potential and for which the lifetime (40 ns) is still quite short.

**Table 5.** Lifetime results for highly excited levels in Ba I

Energy (cm <sup>-1</sup> )	Level	Lifetime (ns)			
		Atomic beam linewidth <sup>D</sup>	Dynamic Stark effect <sup>E</sup>	Laser-induced fluorescence Stepwise <sup>F</sup>	2-photon <sup>F</sup>
34371	6s8s <sup>1</sup> S <sub>0</sub> <sup>A</sup>	8.4(6)		18.2(8)	18.2(8)
34494	6p6p <sup>3</sup> P <sub>0</sub> <sup>B</sup>	5.1(5)	6.4(5)	6.1(5)	6.2(4)
35344	6s7d <sup>1</sup> D <sub>2</sub> <sup>C</sup>	5.9(4)		7.0(5)	6.9(5)
37435	6s8d <sup>1</sup> D <sub>2</sub> <sup>C</sup>	13.2(1.4)			19.7(9)
39335	6s9d <sup>1</sup> D <sub>2</sub> <sup>B</sup>				26.0(1.5)    33(2) <sup>H</sup>
39998	6s10d <sup>1</sup> D <sub>2</sub> <sup>B</sup>			40(3)	43.3(1.4) <sup>G</sup>

<sup>A</sup> Designation according to Rubbmark *et al.* (1977).<sup>B</sup> Designation according to Moore (1958).<sup>C</sup> Designation according to Aymar and Robaux (1979).<sup>D</sup> Deduced from linewidth of laser atomic beam data (Jitschin and Meisel 1980).<sup>E</sup> Fisk *et al.* (1986).    <sup>F</sup> Present work.<sup>G</sup> Kaiser *et al.* (1978).    <sup>H</sup> Leonard and Rinkleff (1985).

Our preliminary data for barium support the result of Fisk *et al.* (1986) for the 6p6p <sup>3</sup>P<sub>0</sub> level, deduced from studies of the dynamic Stark effect, and the laser-induced fluorescence results of Kaiser *et al.* (1978). The result for the 6p6p <sup>3</sup>P<sub>0</sub> level is of particular interest (see e.g. Alford *et al.* 1985; Fisk *et al.* 1986) since this is the uppermost level of the simple  $J = 0 \rightarrow J = 1 \rightarrow J = 0$  'ladder' system, in which both transitions (553.5 and 613.1 nm) lie within the tuning range of rhodamine dyes. The lifetimes of Jitschin and Meisel (1980) (column 3), which were deduced from linewidths of laser atomic beam data, would appear to be systematically short, probably because of contributions from extraneous line broadening.

### Acknowledgments

We are grateful to Drs H.-A. Bachor and P. T. H. Fisk (Australian National University) for drawing our attention to the discrepancy in the lifetime for the Ba 6p6p <sup>3</sup>P<sub>0</sub> level and for assistance with some of the Ba measurements.

### References

- Alford, W. J., Andersen, N., Belsley, M., Cooper, J., Warrington, D. M., and Burnett, K. (1985). *Phys. Rev.* **31**, 3012–16.
- Andersen, T., Ramanujam, P. S., and Bahr, K. (1978). *Astrophys. J.* **223**, 344–9.
- Aymar, M., and Robaux, O. (1979). *J. Phys. B* **12**, 531–46.
- Biémont, E., Grevesse, N., Hannaford, P., and Lowe, R. M. (1981). *Astrophys. J.* **248**, 867–73.
- Biémont, E., Grevesse, N., Hannaford, P., Lowe, R. M., and Whaling, W. (1983). *Astrophys. J.* **275**, 889–91.
- Blagoev, K. B., Komarovskii, V. A., and Penkin, N. P. (1977). *Opt. Spectrosc. (USSR)* **42**, 238–9.
- Blaise, J., Morillon, C., Schweighofer, M. G., and Verges, J. (1969). *Spectrochim. Acta B* **24**, 405–45.
- Brand, H. (1978). Ph.D. Thesis, University of Hannover.
- Brand, H., Drake, K. H., Lange, W., and Mlynek, J. (1980). *Phys. Lett. A* **75**, 345–7.
- Brault, J. W. (1976). *J. Opt. Soc. Am.* **66**, 1081.
- Carrington, C. G., and Corney, A. (1971). *J. Phys. B* **4**, 849–68.

- Corliss, C. H., and Bozman, W. R. (1962). 'Experimental Transition Probabilities for Spectral Lines of Seventy Elements', NBS Monograph No. 53 (U.S. Govt Printing Office: Washington, D.C.).
- Delbouille, L., Neven, L., and Roland, G. (1973). 'Photometric Atlas of the Solar Photospheric Spectrum from  $\lambda$ 3000 to  $\lambda$ 10000 (Institute of Astrophysics, University of Liège).
- Duquette, D. W., Salih, S., and Lawler, J. E. (1981). *Phys. Lett. A* **83**, 214–16.
- Duquette, D. W., Salih, S., and Lawler, J. E. (1982). *Phys. Rev. A* **25**, 3382–4.
- Dyall, K. G. (1986). *Aust. J. Phys.* **39**, 667–78.
- Fisk, P. T. H., Bachor, H.-A., and Sandeman, R. J. (1986). *Phys. Rev. A* **33**, 2418–23.
- Fuhr, J. R., Miller, B. J., and Martin, G. A. (1978). 'Bibliography on Atomic Transition Probabilities (1914 through October 1977)', NBS Special Publn 505 (U.S. Govt Printing Office: Washington, D.C.).
- Fuhr, J. R., Miller, B. J., and Martin, G. A. (1980). 'Bibliography on Atomic Transition Probabilities (November 1977 through March 1980)', NBS Special Publn 505, Suppl. 1 (U.S. Govt Printing Office: Washington, D.C.).
- Gough, D. S., Hannaford, P., and Lowe, R. M. (1982). *J. Phys. B* **15**, L431–4.
- Gough, D. S., Hannaford, P., and Lowe, R. M. (1983). *J. Phys. B* **16**, 785–91.
- Grant, I. P. (1986). *Aust. J. Phys.* **39**, 649–65.
- Handrich, E., Steudel, A., Wallenstein, R., and Walther, H. (1969). *J. Phys. (Paris)* **30**, Suppl. 1, 18–23.
- Hannaford, P., Larkins, P. L., and Lowe, R. M. (1981). *J. Phys. B* **14**, 2321–7.
- Hannaford, P., and Lowe, R. M. (1981). *J. Phys. B* **14**, L5–9.
- Hannaford, P., and Lowe, R. M. (1982). *J. Phys. B* **15**, 65–8.
- Hannaford, P., and Lowe, R. M. (1983a). *Opt. Eng.* **22**, 532–44.
- Hannaford, P., and Lowe, R. M. (1983b). *J. Phys. B* **16**, 4539–42.
- Hannaford, P., and Lowe, R. M. (1983c). *J. Phys. B* **16**, L43–6.
- Hannaford, P., and Lowe, R. M. (1985). *J. Phys. B* **18**, 2365–70.
- Hannaford, P., Lowe, R. M., Biémont, E., and Grevesse, N. (1985). *Astron. Astrophys.* **143**, 447–50.
- Hannaford, P., Lowe, R. M., Grevesse, N., Biémont, E., and Whaling, W. (1982). *Astrophys. J.* **261**, 736–46.
- Jitschin, W., and Meisel, G. (1980). *Z. Phys. A* **295**, 37–43.
- Kaiser, D., Kulina, P., Livingston, A. E., Radloff, H.-H., and Tudorache, S. (1978). *Z. Phys. A* **285**, 111–14.
- Kock, M., and Richter, J. (1968). *Z. Astrophys.* **69**, 180–92.
- Kulina, P., and Rinkleff, R.-H. (1985). *Z. Phys. A* **321**, 15–21.
- Kwiatkowski, M., Micali, G., Werner, K., and Zimmermann, P. (1981). *Phys. Lett. A* **85**, 273–4.
- Leonard, C., and Rinkleff, R.-H. (1985). *Phys. Lett. A* **112**, 208–10.
- Luypert, R., and Van Craen, J. (1977). *J. Phys. B* **10**, 3627–36.
- McLean, R. J., Gough, D. S., and Hannaford, P. (1985). 'Laser Spectroscopy VII' (Eds T. W. Hänsch and Y. R. Shen), p. 220 (Springer: Heidelberg).
- Migdalek, J., and Baylis, W. E. (1978). *J. Phys. B* **11**, L497–501.
- Migdalek, J., and Baylis, W. E. (1979). *J. Quant. Spectrosc. Radiat. Transfer* **22**, 113–25.
- Mlynek, J., and Lange, W. (1979). *Opt. Commun.* **30**, 337–40.
- Mlynek, J., Tamm, Chr., Buhr, E., and Wong, N. C. (1984). *Phys. Rev. Lett.* **53**, 1314–17.
- Moore, C. E. (1958). 'Atomic Energy Levels', NBS Circular No. 467 (U.S. Govt Printing Office: Washington, D.C.).
- Parigger, C., Hannaford, P., Sandle, W. J., and Ballagh, R. J. (1985). *Phys. Rev. A* **31**, 4043–6.
- Penkin, N. P., and Komarovskii, V. A. (1976). *J. Quant. Spectrosc. Radiat. Transfer* **16**, 217–52.
- Poulsen, O., Andersen, T., Bentzen, S. M., and Nielsen, U. (1981). *Phys. Rev. A* **24**, 2523–31.
- Raj, R. K., Köster, E., Gao, Q. F., Camy, G., Bloch, D., and Ducloy, M. (1983). 'Laser Spectroscopy VI' (Eds H. P. Weber and W. Lüthy), pp. 122–7 (Springer: Heidelberg).
- Ramanujam, P. S. (1977). *Phys. Rev. Lett.* **39**, 1192–4.
- Rubbmark, J. R., Borgström, S. A., and Bockasten, K. (1977). *J. Phys. B* **10**, 421–32.
- Rudolph, J., and Helbig, V. (1982a). *J. Phys. B* **15**, L599–602.
- Rudolph, J., and Helbig, V. (1982b). *Z. Phys. A* **306**, 93–4.

- Whaling, W., Hannaford, P., Lowe, R. M., Biémont, E., and Grevesse, N. (1984). *J. Quant. Spectrosc. Radiat. Transfer* **32**, 69-80.
- Whaling, W., Hannaford, P., Lowe, R. M., Biémont, E., and Grevesse, N. (1985). *Astron. Astrophys.* **153**, 109-15.

Manuscript received 12 March, accepted 30 April 1986